LONG DISTANCE LASER ULTRASONIC PROPAGATION IMAGING SYSTEM WITH DAMAGE VISUALIZATION TECHNIQUES

D. Dhital[1], J.R.Lee[1]*, H.J. Shin[1]
[1] Smart Structures Lab, Chonbuk National University 567 Baekje-daero, 561-756, Deokjin-gu, Jeonju, Republic of Korea
* Corresponding author(leejrr@jbnu.ac.kr)

Keywords: *laser ultrasound, ultrasonic propagation imaging system, damage visualization, acoustic emission sensor, collimator*

Abstract
This study proposes a portable long distance laser ultrasonic propagation imaging (LUPI) system with associated damage visualization algorithms based on anomalous wave propagation imaging (AWPI) methods with adjacent wave subtraction, reference wave subtraction, reference image subtraction, and the variable time window amplitude mapping (VTWAM) for a robust SHM solution.

1 Introduction

Wind turbine blade failure is one of the prominent and most common types of damage occurring in operating wind turbine systems [1]. It accounts for about 15-20% of the total turbine cost [2]. The conventional NDE systems are expensive and difficult for in-situ application in wind turbine blades. Thus, we have proposed a portable long distance laser ultrasonic propagation imaging (LUPI) system with beam expander/collimator for long range scanning application that uses a laser beam targeting and scanning system to excite, from a long distance and acoustic emission sensors installed in the blade for sensing. To develop a reliable damage evaluation system, the excitation/sensing technology and the associated damage visualization algorithm are equally important. Hence, our results provide a new platform based on anomalous wave propagation imaging (AWPI) methods with adjacent wave subtraction, reference wave subtraction, reference image subtraction, and the variable time window amplitude mapping (VTWAM) method. Long distance scanning at a distance of 40 m with damage detection and visualization was successfully conducted on a mock up blade leading edge specimen with a 20 mm disbond as shown in Fig. 1.

2 Portable long distance UPI system

The portable components can be installed in the tower as shown in Fig. 2. and the entire UPI system could be categorized into three parts: 1) long distance laser ultrasonic excitation and beam scanning, 2) fixed ultrasonic reception, and 3) the damage visualization process. A schematic diagram of the entire system configuration is shown in Fig. 3. The Q-switched DPSS laser (QL), a laser beam expander/collimator, a galvanometric laser mirror scanner (LMS) and the LMS rotator constitute the laser beam targeting and scanning system. Acoustic emission (AE) sensors embedded in the inner walls of the blades, especially at damage hot spots such as leading edge, trailing edge, and spar bond lines, provide ultrasonic reception under the active sensing scheme. The filters, digitizer, and computer hardware are used for damage evaluation and visualization.

3 Laser beam collimation effect

Without collimation, our DPSS laser with a beam divergence angle of 1.6 mrad and an initial beam diameter of 0.7 mm gives a beam diameter of 64.7 mm at L=40 m. The laser energy density decreases dramatically and the spatial resolution becomes unsuitable for scanning ultrasonic inspection. A Galilean beam expander /collimator was used, which collimated the laser beam after a ten-fold expansion, and maintained the collimated beam diameter and laser energy density adequately for ultrasonic generation at a long distance. After using the Galilean beam expander/collimator, beam diameter is reduced to 13.4 mm while it also provides with an increment in the amplitude of the ultrasonic wave

signal for the long distance excitation at 40 m. An experimental study was done which showed that the signal strengths of S0 and the A0 mode at 40 m for the collimated laser beam were higher by 41.5 dB and 23.1 dB, respectively, compared to the un-collimated results.

4 Damage visualization algorithms

Ultrasonic wave propagation imaging is successful in simple structures [3] but provides with low damage visibility in complex structures. Therefore, it is difficult even for skilled inspectors to identify a defect accurately using received waveforms within a short time. The realistic imaging of ultrasound propagation in structures helps us understand the interrelation between the complex behavior of ultrasound in structures and the waveforms that appear on a monitor. Realistic imaging eases the interpretation of damage evaluation results, and increases the accuracy of detection through visualization. New algorithms for AWPI and VTWAM methods have been developed for enhanced result processing algorithm for the LUPI system, with improved damage visibility.

4.1 Adjacent wave subtraction algorithm

The AWPI method with adjacent wave subtraction was developed as an advanced and enhanced results-processing algorithm for the LUPI system as presented in [4]. In this algorithm, the self-normalized signal from the current laser impinging point is subtracted by that from the prior adjacent point acquired just before the signal, and the process continues for each laser impinging point over the entire scanning area. The differences between the two adjacent waves are minimized by shifting one wave along the time axis by a few multiples of the wave-sampling intervals. It is a spatial referencing algorithm that was proposed to eliminate the adverse effects of temporal referencing and to improve low damage visibility results from the conventional ultrasonic wave propagation imaging (UWPI) movie in complex structures. The adjacent wave subtraction AWPI algorithm highlights anomalous waves due to damage and material discontinuity, and enhances the visibility of damage by suppressing the incident waves. Therefore, a damage-induced anomalous wave can be easily identified, even for complex structures.

The adjacent wave subtraction algorithm involves three cases of signal interaction (far, near, and at the damage). When the laser impingement points are far from a structural anomaly, two adjacent waves that do not contain anomalous waves are generated. When the signal from a current laser impingement point (the i^{th} point) is subtracted by the signal acquired from the laser impingement point just before the current point (the $i-1^{th}$ point), the subtracted signal, minimized in terms of root mean square error by wave shifting and amplitude normalization, has no anomalous wave or is near the noise floor. At or near the damage, where the wave interaction changes due to the anomaly, the subtraction yields some residue around the incident wave part, and the anomalous waves such as scattering and confining waves. Processing of the adjacent wave subtraction AWPI could be carried out during the scan. To generate the adjacent wave subtraction AWPI movie, the subtracted signals are stored as one row of data in a spreadsheet. Any of these spreadsheets plotted on an intensity map with a suitable color scheme is a freeze-frame from the AWPI movie. An AWPI movie can be generated by displaying the freeze-frames in succession, at a refresh rate similar to a video. The adjacent wave subtraction AWPI has the important merit of the temporal reference-free method. Adjacent wave subtraction AWPI does not need reference state data, and provides an enhancement to damage visualization compared to the conventional UWPI. On the other hand, clearer damage information can be provided if ultrasonic wave propagation signals in a reference state are available. Therefore, the new platform for the LUPI system includes two more AWPI algorithms, reference wave subtraction and reference image subtraction, which are described as follows.

4.2 Reference wave subtraction algorithm

For AWPI based on reference subtraction algorithm, reference data from the target specimen is already collected in its intact state (e.g., the previous inspection data in the pre-scheduled inspections), and is used as a reference for subtraction of signals during AWPI process. The reference and current state waves are self-normalized, and the signal from the laser impingement point at a particular location in the reference data is subtracted from the signal from the same point in the current scanning data.

Differences between the reference and current state waves are minimized by shifting one wave along the time axis by a few multiples of wave sampling intervals. In other words, the reference state wave and current state wave are used instead of the two adjacent waves in the spatial domain. The AWPI movie generation process is then the same as previously described for adjacent wave subtraction.

4.3 Reference image subtraction algorithm

It is another temporal referencing-based technique where the reference data at the intact state is also used as the reference for the subtraction algorithm. The concept used for the reference image subtraction AWPI method is to conduct image-by-image subtraction between the reference and current states. However, if the current scanning area does not perfectly overlap with the reference, the generated freeze-frame at each signal sampling point will be slightly biased from the estimated optimum result. An image-by-image subtraction under this condition might produce freeze-frames with a high residual of incident waves due to pixel mismatch. Hence, in the reference image subtraction AWPI algorithm, to avoid a high residual of incident waves due to the pixel mismatch, image matching is first performed within the algorithm. For image matching, the algorithm selects a freeze-frame from the current state at a particular time point, and is subtracted with another freeze-frame at the same time point from the reference state. The time point can be an arbitrary time point after the appearance of the anomalous wave. Or, if fully automatic operation is preferred, it can be set as the middle point of the signal sampling period. For the same freeze-frames, several variations of horizontal and vertical sweeps are performed during the subtraction, thereby producing a new set of images as shown in Fig. 4.

The default deviation in pixel value p is ±5 pixels, which generates $(2p+1)^2$ subtracted images. For a typical inspection case with a laser grid interval of 1.0 mm, this value of p corresponds to a deviation of 5 mm between the reference and current states. Therefore, inspection area mismatch between the reference and current state scans can be allowed by the image matching algorithm. The optimum matching condition at a particular sweep distance produces an image with minimum root mean square error, which results in low incident wave residue but high anomalous wave residue; i.e., a damage-induced anomalous wave. Then, the reference image subtraction algorithm with the particular sweep as the optimum matching measure is applied to all the freeze-frames throughout the sampling time points. The resulting freeze-frames are appended into the new data structure, and the resulting data from the spreadsheets generates an AWPI movie.

4.4 Variable time window amplitude map

For structures with complex features such as aircraft wing box with stiffeners and highly anisotropic structures, we propose VTWAM to further enhance the damage visibility which is based on the difference in the appearance time between the residues of the incident wave and the damage-induced anomalous wave. An amplitude map based on the VTWAM method enhances damage visualization and facilitates damage size evaluation. Conventional amplitude mapping methods map the maximum peak-to-peak amplitude of all the subtracted signals to an image using a full time window. In actual practice, despite signal subtraction, the amplitude near the sensing point could be potentially higher than the amplitudes of the damage-induced anomalous waves. This problem can be solved by selecting a suitable time window in the AWPI movie. The starting time for the window is selected so as to include only the portion after the encounter of structural damage of the incident wave because the damage-induced anomalous wave is only generated by the incident wave sweep.

5 Leading edge inspection of a composite blade specimen

To investigate the efficiency of the proposed long distance damage evaluation system, tests were conducted on a composite wind turbine blade specimen. A leading edge specimen was used in the test because it is one of the most important damage hotspots for turbine blades, and it has a complex curved surface geometry. The specimen was made from two pieces of carbon fiber reinforced plastic (CFRP) plate bonded to form an angle 115°, as shown in Fig. 1. The size of each plate is 300 mm × 200 mm × 5 mm. A 20 mm region at the center of the specimen was not bonded to simulate leading edge disbond. A 1.5 mJ laser with a 1 kHz repetition rate was used to scan a 200 mm × 200 mm area with

a scanning spatial interval of Δ=0.5 mm. Ten-fold amplification and 100 to 200 kHz bandpass filtering was used during signal acquisition, and spatial averaging with a 3×3 kernel was applied twice during post-image processing.

Damage visualization results

In the AWPI process, adjacent wave subtraction, reference wave subtraction, and reference image subtraction algorithms were used. The ultrasonic incident waves were highly suppressed with only the leading edge disbond as shown in Figs. 5 (a)-(c). Since these algorithms became much more sensitive to a damage-induced wave than conventional UWPI movie, they greatly enhanced damage visibility, and provided damage location and size information that were easily distinguishable. The disbond was visible after 25 μs, which could readily be seen without the need for further visual analysis. In VTWAM process, then, a suitable time window selection was needed to generate the amplitude map. The time window size should be selected such that it includes only the portion of signals after the encounter of structural damage by the incident ultrasonic wavefield. The incident ultrasonic wave reached the leading edge after 25.2 μs, as determined from the AWPI movies. Hence, a time window from 25 μs to the end of wave, 188 μs was selected for the VTWAM method, as shown in Figs. 6 (a)-(c). The amplitude was found to be concentrated at the disbond region. Both the AWPI and VTWAM algorithms provided uniform and precise damage location information, as shown in Figs. 5 and 6.

Then, a comprehensive comparison of damage visualization algorithms was made through performance analysis; i.e., SNR calculations and the accuracy of damage size detection. The results, presented in Fig. 7, show a close correlation to the accuracy of the calculated damage size evaluation and the actual disbond length. The disbond size, based on the results, ranged between 19.02 and 23.08 mm. These values are in close agreement with the actual damage size of 20 mm. The algorithms were further analyzed and compared on the basis of SNR calculations. The noise was estimated from the far field region in the amplitude maps as shown in Fig. 6, and the observation was four standard deviations (4σ) away from the noise mean, representing 99.99% confidence of noise rejection. Comparative analysis results and a summary of general advantages and disadvantages are given in Table 1.

All three AWPI algorithms and the VTWAM method provide enhanced results with distinct advantages compared to the conventional UWPI algorithm. The adjacent wave subtraction AWPI is a reference-free on-site inspection algorithm that does not need temporal referencing. Thus, it is useful when reference data is not available. On the other hand, the reference wave subtraction AWPI could not present a higher SNR than that of the adjacent wave subtraction AWPI. Nonetheless, the reference image subtraction AWPI provided an amplitude map with SNR that was 8.82 dB higher. Since a possible scan area mismatch between reference data (previous inspection) and current inspection data can be automatically solved by the image matching technique in the reference image subtraction AWPI algorithm itself, the reference image subtraction AWPI is preferable if reference data is available.

Conclusion

A portable LUPI system for long distance laser ultrasonic excitation/sensing was for long distance in-situ wind turbine applications. The LUPI system in combination with the AWPI and VTWAM algorithms provided enhanced results for damage visibility, and high accuracy in determining damage location and size. The results demonstrated the possibility of quantitative damage evaluation and enhanced visualization for in situ turbine blades at long distances. Thus, the proposed LUPI system showed excellent application feasibility, and could offer a robust SHM solution for in-field long distance applications in wind turbine systems.

Acknowledgement

This work was supported by a New and Renewable Energy grant from the Korea Institute of Energy Technology Evaluation and Planning (KETEP), funded by the Ministry of Knowledge Economy of the Korean government (2008-N-WD08-P-01-0000 and 20103020020010). This paper was also supported by Korea Ministry of Land, Transport and Maritime Affairs as Haneul Project. The authors gratefully acknowledge this support.

Table. 1. Comparison of damage visualization algorithms based on SNR calculations and accuracy of damage size detection with generalized advantages and disadvantages (AWPI: anomalous wave propagation imaging, VTWAM: variable time window amplitude mapping)

AWPI algorithms + VTWAM	Performance		Advantages	Disadvantages
	SNR	Damage size evaluation		
Adjacent wave subtraction	16.01 dB	19.02 mm	Reference data not required, high accuracy for damage size evaluation	Comparatively lower SNR
Reference wave subtraction	12.43 dB	20.98 mm	High accuracy for damage size evaluation	Reference data required, comparatively lower SNR
Reference image subtraction	24.84 dB	23.08 mm	Comparatively higher SNR, image matching can reduce the effect of scan area mismatch	Reference data required, comparatively lower accuracy for damage size evaluation

Figures

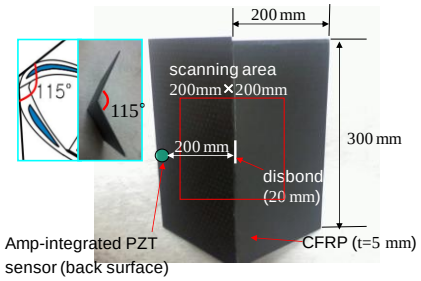

Fig. 1. Mock-up of blade leading edge.

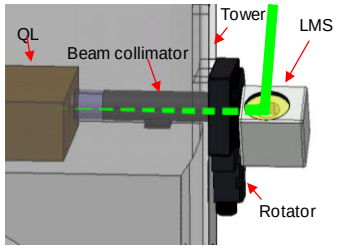

Fig. 2. The long distance UPI system.

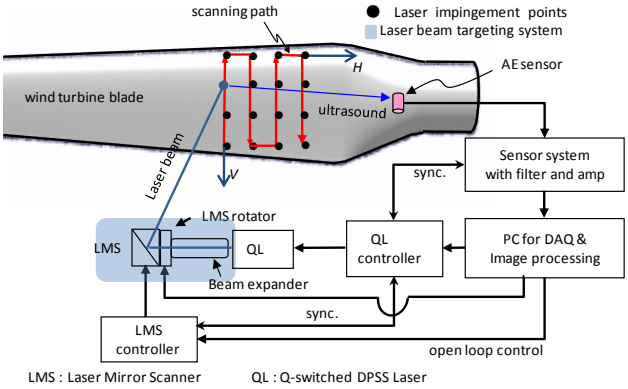

Fig. 3. Portable UPI system configuration for long distance application.

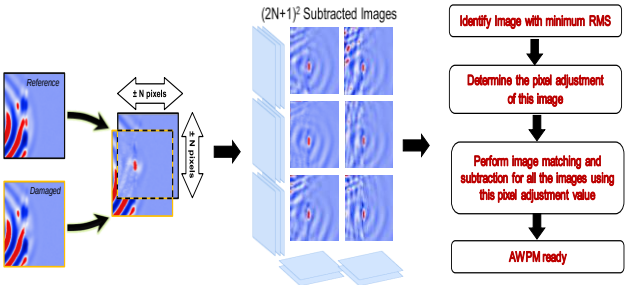

Fig. 4. Reference image subtraction algorithm with image matching technique.

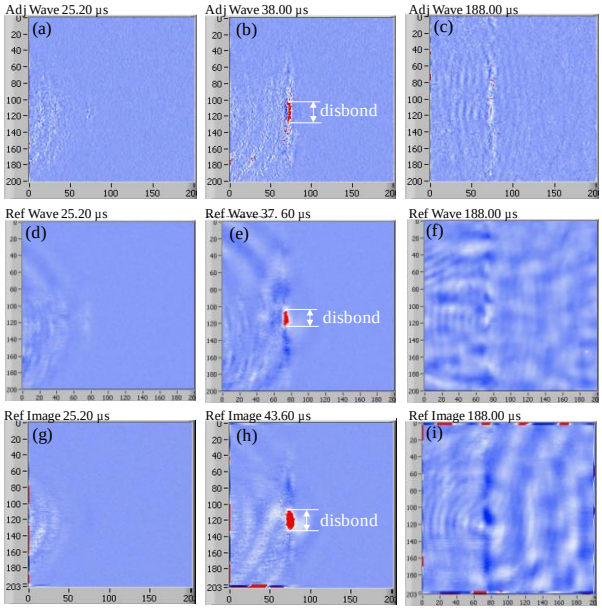

Fig. 5. AWPI movie freeze frames at different time intervals and visible disbond region. (a)-(c) adjacent wave subtraction. (d)-(f) reference wave subtraction. (g)-(i) reference image subtraction algorithm.

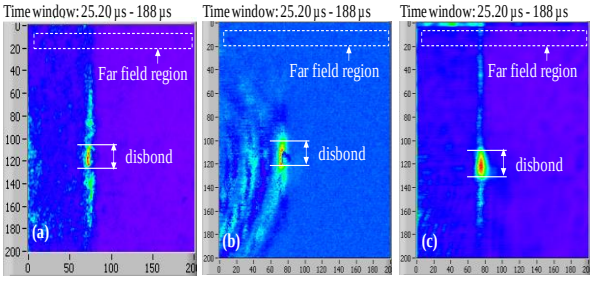

Fig. 6. Amplitude maps processed by VTWAM method based on (a) adjacent wave subtraction, (b) reference wave subtraction, and (c) reference image subtraction algorithm.

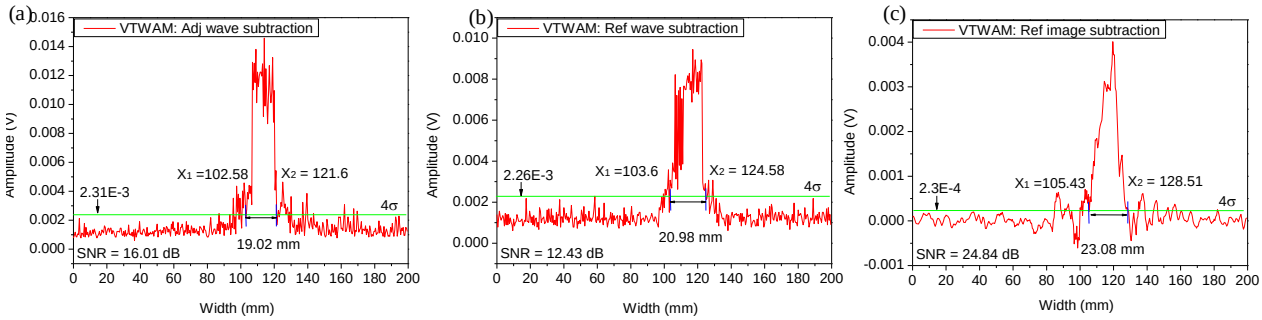

Fig. 7. Comparative analysis based on damage size evaluation accuracy and SNR. The VTWAM algorithms are based on (a) adjacent wave subtraction, (b) reference wave subtraction, and (c) reference image subtraction.

References

[1] M.M. Khan, M.T. Iqbal and F. Khan "Reliability analysis of a horizontal axis wind turbine". *IEEE 14th NECEC conference*, Newfoundland, Canada, 2004.

[2] F.M. Larsen and T. Sorensen "New lightning qualification test procedure for large wind turbine blades". *Proceedings of International Conference on Lightning and Static Electricity*, Blackpool, UK, pp 36.1–10, 2003.

[3] C.C. Chia, J.R. Lee, J.S. Park, C.Y. Yun and J.H. Kim "New design and algorithm for an ultrasonic propagation imaging system". *Proceedings of International Conference of DEFEKTOSKOPIE*, Brno, Czech, pp 63-70, 2008.

[4] J.R. Lee, J. Takatsubo, N. Toyama and D.H. Kang "Health monitoring of complex curved structures using an ultrasonic wavefield propagation imaging system" *Meas. Sci. Technol.* Vol. 18, pp 3816–24, 2007.